

## SPATIAL MODEL OF LANDSLIDE HAZARD IN TARUSAN WATERSHED

Triyatno\*<sup>1</sup>, Iswandi, U\*<sup>1</sup>, Febriandi\*<sup>1</sup>

\*<sup>1</sup>Department of Geography, FIS Padang State University

\*Corresponding Author, Received: August 20, 2022. Revised: Nov 21, 2022. Accepted: Dec 26, 2022

**Abstract:** *Spatial modeling of landslide hazards in the Tarusan watershed is an effort to reduce losses due to landslide disasters. The purpose of this article is; determine the frequency ratio value of each parameter that causes landslides, and perform spatial modeling of landslide hazards using the frequency ratio method. The method used is a quantitative method with a modeling approach to determine the pixel value based on the frequency ratio. The results of the research show that the largest frequency value is found in the land cover parameter in the form of mixed gardens with an FR value of 2, 10, and rainfall with an FR value of 2.06. Thus, the triggering factors for landslides in the Tarusan watershed are changes in land cover and rainfall. The results of landslide hazard modeling in the Tarusan watershed show a high hazard area of 2095.41 ha or 7.39%, a medium hazard area of 4148.73 ha or 14.63%, and a low hazard area of 22117.46 ha or 77.98%.*

Key words: hazard, landslide, spatial model

### 1. Introduction

The intensity of natural disasters lately tends to increase, this is caused by natural and non-natural factors, [3,6,8,12]. Many natural factors that cause disasters are global climate change, while non-natural factors that trigger natural disasters are human intervention on nature, [5,9,14,16]. Human intervention on the environment is mostly caused by the urge to fulfill the needs of human life, so that humans do a lot of land functions to meet the needs of life, [10,14,16].

Uncontrolled land conversion often triggers natural disasters in the form of microclimate changes, land degradation, floods, droughts, and landslides. The method used in this research is quantitative using remote sensing basic data and shape file data in ArcGis software to convert to raster data which is the main requirement in the modeling process, [1,2,8]. The sample in this study is in the form of everything

$$N = N / (1 + (N \times e^2))$$

Where:

n = number of samples

N = total population (pixels)

E = precision

To determine the size of the sample class, the formula proposed by [1,2] is as follows;

$$ni = \frac{Ni}{N} \cdot n$$

Where;

ni = number of sample members by class

Ni = number of population members by class

[4,7,11,13]. Landslide natural disasters have caused many losses, both property and human loss, [6,15,18,]. One of the areas that experienced natural landslides is the Tarusan watershed which is located in the western part of the island of Sumatra. Tarusan watershed is a connecting route that connects the cities of Padang and Painan and Bengkulu Province, [3,4,]. The impact of the landslide natural disaster in this area was the disconnection of the land route connecting Padang City to Painan and Bengkulu Province, especially for the flow of goods and people. The impact of natural disasters from landslides also caused fallen trees and casualties.

### 2. Research Method

contained in the Tarusan watershed with the population in the form of the number of pixels from the modeling results. To determine the size of the research sample, it is determined based on the formula as follows;

N = total population

n = total number of sample members

To determine the landslide hazard model, the frequency ratio proposed by [5,14] has the following formulation;

$$Fr = \frac{nNpix(1)/Npix(2)}{\sum Npix(3)/\sum Npix(4)}$$

Where;

Fr = frequency ratio

Npix (1) = number of pixels containing landslides in class i

Npix (2) = total number of pixels from each class in the entire area  
 Npix(3) = total number of pixels containing landslide  
 Npix4) = total number of pixels in the study area.  
 To determine the landslide hazard class, the following formula is used;  
 $Lhm = 0.25*fr1+0.25*Fr2+0.20*Fr3+0.10*Fr4+0.10*fr5+0.6*Fr6$   
 Where;  
 Fr= frequency ratio  
 N = constant number of selected landslide-causing factors

accuracy, and producer accuracy is used with the formula proposed by [1,2,17] as follows;

$$User\ accuracy = \frac{x_{ii}}{x_{+i}} \times 100\%$$

$$roducer\ accuracy = \frac{x_{ii}}{x_i + \sum_i^r x_{ii}} \times 100\%$$

$$Overall\ accuracy = \frac{\sum_i^r x_{ii}}{N} \times 100\%$$

Where;

Xii = the diagonal value of the ith row and ith column contingency matrix

Xi = number of pixels in row\_i

X + = Number of pixels in column i

N = number of pixels in sample

### 3. Results and Discussion

To determine the accuracy of the landslide hazard model, an accuracy test using overall accuracy, user  
 To determine the landslide hazard model in the research area, the frequency ratio value of the slope, soil, rainfall, geology, geomorphology, and land

cover parameters is used. For more details can be seen in the following table;

Table 1. Frequency Ratio of Slope for Tarusan Watershed Class

Slope class	Number of pixel	Percentage (%)	Landslide pixel	Percentage (%)	FR
flat	45.697	14,50	123	0,06	0,00
sloping	6.396	2,03	3.258	1,54	0,76
Medium	87.284	27,70	38.778	18,32	0,66
steep	154.292	48,96	153.464	72,50	1,48
Very steep	21.460	6,81	16.048	7,58	1,11
Total	315.129	100,00	211.671	100,00	4,02

Source; 2021 Data Analysis

The table above shows that the highest slope frequency ratio value is 1.48 which is found in the

steep slope class and the lowest is 0, which is found on the flat slope.

Table 2. Frequency Ratio of Soil Type in Tarusan Watershed

Soil type	Number of pixel	Percentage (%)	Number of pixel	Percentang (%)	FR
Andosol	118.508	37,61	33.571	48,28	1,28
Latosol	47.128	14,96	7.335	10,55	0,71
Litosol	107.944	34,25	28.615	41,15	1,20
Alluvial	41.550	13,19	9	0,01	0,00
Total	315.129	100,00	69.529	100,00	3,19

Source; 2021 Data Analysis

The highest FR value is 1.28 which is found in the Andosol soil type and the lowest with an FR value of 0.00 is found in the alluvial soil type.

Table 3. Frequency Ratio of Rainfall in Tarusan Watershed

Rain fall (mm)	Number of pixel	percentage (%)	Number of pixel	percentage (%)	FR
1500 - 2000	16.439	5,22	7.491	10,76	2,06
2000 - 2500	193.920	61,54	46.444	66,72	1,08
2500 - 3000	98.736	31,33	15.659	22,50	0,72
> 3000	6.035	1,91	12	0,02	0,01
Total	315.129	100,00	69.606	100,00	3,87

Source; 2021 data analysis

The highest FR value of rainfall is 2.06 which is found in areas with rainfall ranging from 1,500 – 2,000 mm/year, and the lowest with an FR value of

0.01 which is found in areas with rainfall > 3,000 mm/year.

Table 4. Frequency Ratio of Rock Types in Tarusan Watershed

Geology type	Number of pixel	Percentage (%)	Landslide pixel	Percentage (%)	FR
Alluvium	38.990	12,37	45	0,06	0,01
Breccia	144.633	45,90	22.310	31,86	0,69
Extrusif intermediate Polymict	60.126	19,08	24.228	34,60	1,81
IntrusifFesicGranitoid	27.834	8,83	4.208	6,01	0,68
Quarzite	43.547	13,82	19.230	27,46	1,99
Total	315.129	100,00	70.020	100,00	5,18

Source; 2021 data analysis

The highest FR value for geological conditions in the study area is 1.99, which is Quarzite rock type and the lowest is 0.01 in alluvium rock.

Table 5. Frequency Ratio of Landform Unit of the Tarusan Watershed

Landform unit	Number of pixel	Percentage (%)	Landslide pixel	Percentage (%)	FR
Dataranaluvial	40.066	12,71	5	0,01	0,00
Perbukitan Vulkanik	44.159	14,01	6.335	9,07	0,65
Pegunungan Vulkanik	230.905	73,27	63.539	90,93	1,24
Total	315.129	100,00	69.879	100,00	1,89

Source; 2021 Data Analysis

The highest FR value of the landform unit is 1.24 which is found in the volcanic mountain landform unit, and the lowest is found in the alluvial plain landform unit with an FR value of 0.00.

Table 6. Frequency Ratio of Land Cover Tarusan Watershed

Land Cover	Number of pixel	percentage (%)	Landslide pixel	Percentage (%)	FR
Primary forest	169.164	53,68	28.049	40,18	0,75
Secondary forest	62.412	19,80	14.698	21,05	1,06
Palm	28	0,01	0	0,00	0,00
Mangrove	39	0,01	0	0,00	0,00
Water body	2.417	0,77	0	0,00	0,00

Build up area	11.221	3,56	1.748	2,50	0,70
Paddy fiel	15.401	4,89	455	0,65	0,13
Dryland farming	1.749	0,55	374	0,54	0,97
Mixed orchard	52.730	16,73	24.492	35,08	2,10
Total	315.161	100,00	69.816	100,00	5,71

Source; Data Analysis Year, 2021

The highest FR value of land cover is 2.10 in mixed garden land cover and the lowest is found in mangrove, oil palm, and water bodies with an FR value of 0.00. The picture frequency ratio can be seen in the following figure;

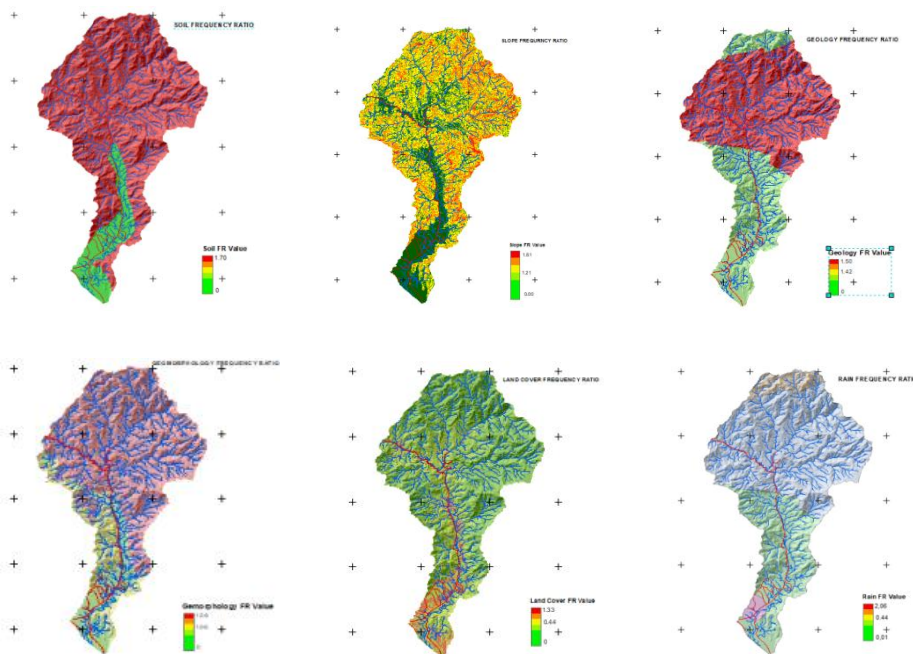


Figure 1. Frequency Ratio Value of Parameters Cause of Landslide  
 Source; 2022 Data Analysis

The picture above shows that the magnitude of the frequency ratio value of several parameters that cause landslides. The high value of the frequency ratio causes the area to have a high potential for landslides. The high value of the frequency ratio indicates that the area has a lot of pixel values for landslide natural disasters and the lower the frequency ratio value indicates that the area has a low potential for landslides. For more details, the results of landslide hazard modeling based on the frequency ratio value can be seen in the following figure;

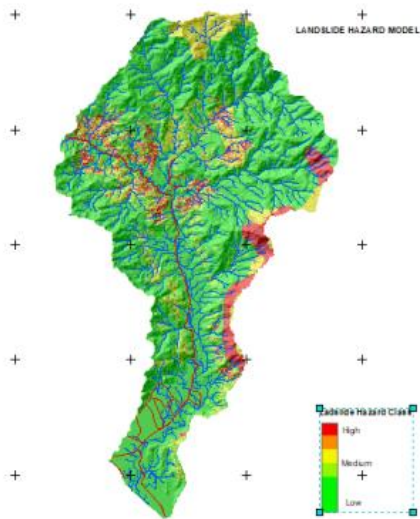


Figure 2. Landslide Hazard Modelling

Source; 2022 Data Analysis

The picture above shows areas that have the potential for landslides in the Tarusan watershed. The area that has a high hazard is 2095.41 ha or 7.39%, an area that has a moderate landslide hazard is 4148.73 ha or 14.63%, and an area that has a low landslide hazard is 22117.46 ha or 77.98%. The data above shows that the Tarusan watershed has an area that has a broad landslide hazard, namely a low hazard, this is because most of the area has flat slopes, and areas that have steep slopes generally have land cover in the form of forest, either forest or forest. primary and secondary forest. The level of landslide hazard in the Tarusan watershed by village or nagari has a different area from one village to another, this is due to the characteristics of the triggering factors for landslides that are different in each village. For more details can be seen in the following table;

Table 7. Landslide Hazard of Tarusan Watershed

No	Village	Landslide Hazard		
		Low	Medium	High
1	AmpangPulai	33.11	0.00	0.00
2	Barung-BarungBalantai Selatan	540.18	129.02	113.71
3	Barung-BarungBalantai Tengah	1203.28	217.06	101.79
4	Barung-BarungBalantaiTimur	1391.63	270.63	293.99
5	Barung-BarungBalantai	881.52	178.08	86.23
6	BatuHampar	378.00	2.89	9.23
7	BatuHampar Selatan	227.53	13.99	1.10
8	Duku Utara	1557.64	227.08	295.57
9	Duku	1166.02	131.54	2.43
10	JinangKampungpansurAmpangPulai	147.16	0.00	0.00
11	KampungBaru Korong Nan Ampek	2138.36	533.21	293.04
12	Kapuh	582.10	30.19	0.00
13	Kapuh Utara	437.44	22.40	0.83
14	Nanggalo	302.96	26.89	0.00
15	PulauKaramAmpangPulai	161.39	0.00	0.00
16	SetaraNanggalo	146.49	0.00	0.00
17	Siguntur	2287.06	531.09	377.54
18	SigunturTua	750.42	210.96	77.36
19	Taratak Sungai Lundang	7785.16	1623.71	442.59
Total		22117.46	4148.73	2095.42

Source; 2022 Data Analysis

The table above shows that each nagari has an area that has different potential for landslide natural disasters. Nagari which has the highest landslide hazard is Nagari Taratak Sungai Lundang with a high landslide hazard area of 442.59 ha. The Nagari which has the widest moderate landslide hazard is Nagari Taratak Sungai Lundang with an area of 1623.71 ha, and the Nagari which has the widest low landslide hazard is also found in Nagari Taratak Sungai Lundang with an area of 7785.16 ha. Nagari Taratak Sungai Lundang has the widest potential low, medium and high landslide hazard in

the Tarusan watershed, this is because the area has a large area and has slopes that vary from flat to very steep slopes, has weathered rocks, and high rainfall and the morphology of the area in the form of volcanic hills and volcanic mountains.

To determine the accuracy of a model, it is necessary to do an accuracy test, where the accuracy test used is in the form of user accuracy, producer accuracy, and overall accuracy. For more details can be seen in the following table; Environmental Disaster Static Spatial Model Accuracy Test Table

Table 8. Landslide Hazard Tarusan Watershed of year 2022

No	1	2	3	Amount	User accuracy
1	25	1	3	29	86,21
2	3	51	5	59	86,44
3	6	3	302	311	97,11
	34	55	310	399	
<i>Producer</i>	75,76	83,61	97,42		
<i>overall accuracy</i>	25+51+302=378/399			94,74	

Source; 2022 Data Analysis

Description: 1 = High, 2 = Medium, 3 = Low

The table above shows that the accuracy test by user accuracy shows the highest value of 97.11%, the accuracy test value by producer accuracy shows the highest value of 97.74%, and the overall accuracy value shows the value of 94.74%. The overall accuracy value of 94.74% indicates that the results of landslide hazard modeling using the frequency ratio are very good.

#### 4. Conclusion

Based on the above description of landslide hazard modeling based on the frequency

ratio that causes landslide hazards in the Tarusan watershed, the following conclusions can be drawn;

1. The highest frequency ratio value is found in land cover in the form of mixed gardens with a frequency ratio value of 2.10 and rainfall 2.06 which is found in rainfall ranging from 1,500-2,000
2. High landslide hazard area of 2095.42 ha or 7.39%, moderate landslide hazard area of 4148.73 ha or 14.63%, and low landslide hazard area of 22117.46 ha or 77.98%.

#### Reference

1. Achour, Y., & Pourghasemi, H. R. (2019). *How do machine learning techniques help in increasing accuracy of landslide susceptibility maps? Geoscience Frontiers*. doi:10.1016/j.gsf.2019.10.001
2. Battistini, A., Rosi, A., Segoni, S., Lagomarsino, D., Catani, F., & Casagli, N. (2017). *Validation of landslide hazard models using a semantic engine on online news. Applied Geography, 82, 59–65*. doi:10.1016/j.apgeog.2017.03.003
3. BPBD Pesisir Selatan, (2020). 4 Units of South Coast Residents' Houses Hit by Landslide. Editor, Saturday 15 February, 2020.
4. BPBD West Sumatra, (2019). This is a Natural Disaster Prone Area in West Sumatra, West Sumatra BPBD
5. Carlà, T., Tofani, V., Lombardi, L., Raspini, F., Bianchini, S., Bertolo, D., Casagli, N. (2019). *Combination of GNSS, satellite InSAR, and GBInSAR remote sensing monitoring to improve the understanding of a large landslide in high alpine environment. Geomorphology*. doi:10.1016/j.geomorph.2019.03.014
6. Casagli, N., Cigna, F., Bianchini, S., Hölbling, D., Füreder, P., Righini, G., Bianchi, M. (2016). *Landslide Mapping and Monitoring by Using Radar and Optical*

- Remote Sensing: Examples from the EC-FP7 Project SAFER. Remote Sensing Applications: Society and Environment*, 4, 92–108. doi:10.1016/j.rsase.2016.07.001
7. Celia dos Santos Alvalá, R., Carvalho de Assis Dias, M., Saito, S. M., Stenner, C., Franco, C., Amadeu, P., Nobre, C. A. (2019). *Mapping Characteristics of at-risk Population to Disasters in the Context of Brazilian Early Warning System. International Journal of Disaster Risk Reduction*, 101326. doi:10.1016/j.ijdr.2019.101326
  8. Chen, W., Panahi, M., Tsangaratos, P., Shahabi, H., Iliá, I., Panahi, S., Ahmad, B. B. (2019). *Applying Population-Based Evolutionary Algorithms and a Neuro-Fuzzy System for Modeling Landslide Susceptibility. CATENA*, 172, 212–231. doi:10.1016/j.catena.2018.08.025
  9. Chen, W., Xie, X., Peng, J., Shahabi, H., Hong, H., Bui, D. T., Zhu, A.-X. (2018). GIS-Based Landslide Susceptibility Evaluation Using a Novel Hybrid Integration Approach Of Bivariate Statistical Based Random Forest Method. *CATENA*, 164, 135–149. doi:10.1016/j.catena.2018.01.012
  10. Confuorto, P., Di Martire, D., Infante, D., Novellino, A., Papa, R., Calcaterra, D., & Ramondini, M. (2019). *Monitoring of Remedial Works Performance on Landslide-Affected Areas Through Ground- and Satellite-Based Techniques. CATENA*, 178, 77–89
  11. Depina, I., Oguz, E. A., & Thakur, V. (2020). Novel Bayesian Framework for Calibration of Spatially Distributed Physical-Based Landslide Prediction Models. *Computers and Geotechnics*, 125, 103660. doi:10.1016/j.compgeo.2020.103660
  12. Drazba, M. C., Yan-Richards, A., & Wilkinson, S. (2018). *Landslide Hazards in Fiji, Managing the Risk and not the Disaster, a Literature Review. Procedia Engineering*, 212, 1334–1338. doi:10.1016/j.proeng.2018.01.172
  13. Gadrani, L., Lominadze, G., & Tsitsagi, M. (2018). *Assessment of Landuse/Landcover (LULC) Change of Tbilisi and Surrounding Area Using Remote Sensing (RS) and GIS. Annals of Agrarian Science*, 16(2), 163–169. doi:10.1016/j.aasci.2018.02.005
  14. Hawas Khan, Muhammad Shafique, Muhammad A. Khan, Mian A. Bacha, Safeer U. Shah, Chiara Calligaris. (2019). *Landslide Susceptibility Assessment Using Frequency Ratio, a Case Study of Northern Pakistan. The Egyptian Journal of Remote Sensing and Space Sciences*, 22 (2019) [.do/10.1016/j.ejrs.2018.03.004](https://doi.org/10.1016/j.ejrs.2018.03.004)
  15. Kaku, K. (2018). *Satellite Remote Sensing for Disaster Management Support: A Holistic and Staged Approach Based on case Studies in Sentinel Asia. International Journal of Disaster Risk Reduction*. doi:10.1016/j.ijdr.2018.09.015
  16. Lu, P., Qin, Y., Li, Z., Mondini, A. C., & Casagli, N. (2019). *Landslide Mapping From Multi-Sensor Data Through Improved Change Detection-Based Markov Random Field. Remote Sensing of Environment*, 231, 111235. doi:10.1016/j.rse.2019.111235
  17. Nepal, N., Chen, J., Chen, H., Wang, X., & Sharma, T. P. P. (2019). *Assessment of Landslide Susceptibility along the Araniko Highway in Poiqu/BhoteKoshi/Sun Koshi watershed Nepal Himalaya .Progress in Disaster Science* 100037. doi:10.1016/j.pdisas.2019.100037
  18. Pollock, W., Grant, A., Wartman, J., & Abou-Jaoude, G. (2019). *Multimodal Method for Landslide Risk Analysis. MethodsX*, 6, 827–836. doi:10.1016/j.mex.2019.04.012
  19. Thi Ngo, P. T., Panahi, M., Khosravi, K., Ghorbanzadeh, O., Karimnejad, N., Cerda, A., & Lee, S. (2020). *Evaluation of Deep Learning Algorithms for National Scale Landslide Susceptibility Mapping of Iran. Geoscience Frontiers*. doi:10.1016/j.gsf.2020.06.013
  20. Youssef, A. M., & Pourghasemi, H. R. (2020). *Landslide susceptibility mapping using machine learning algorithms and comparison of their performance at Abha Basin, Asir Region, Saudi Arabia. Geoscience Frontiers*. doi:10.1016/j.gsf.2020.05.010